

Quantum Mechanical Study of Molecular Weight Growth Process by Combination of Aromatic Molecules

A. VIOLI,*¹ and A. F. SAROFIM

Department of Chemical & Fuels Engineering, University of Utah, Salt Lake City, UT 84112, USA

and

T. N. TRUONG

Henry Eyring Center for Theoretical Chemistry, Department of Chemistry, University of Utah, Salt Lake City, UT 84112, USA

Formation pathways for high-molecular-mass compound growth are presented, showing why reactions between aromatic moieties are needed to explain recent experimental findings. These reactions are then analyzed by using quantum mechanical density functional methods. A sequence of chemical reactions between aromatic compounds (e.g., phenyl) and compounds containing conjugated double bonds (e.g., acenaphthylene) was studied in detail. The sequence begins with the H-abstraction from acenaphthylene to produce the corresponding radical, which then furnishes higher aromatics through either a two-step radical-molecule reaction or a direct radical-radical addition to another aromatic radical. Iteration of this mechanism followed by rearrangement of the carbon framework ultimately leads to high-molecular-mass compounds. This sequence can be repeated for the formation of high-molecular-mass compounds. The distinguishing features of the proposed model lie in the chemical specificity of the routes considered. The aromatic radical attacks the double bond of five-membered-ring polycyclic aromatic hydrocarbons. This involves specific compounds that are exceptional soot precursors as they form resonantly stabilized radical intermediates, relieving part of the large strain in the five-membered rings by formation of linear aggregates. © 2001 by The Combustion Institute

INTRODUCTION

Formation of soot and other carbonaceous material during the incomplete combustion of hydrocarbons is one of the least resolved problems; despite essential progress in understanding single processes, the comprehensive theory and models that predict the formation of these compounds fall short of predicting many of the experimental observations.

The seminal work in this area is due to Frenklach et al. [1–4], who dealt primarily with C₂H₂ pyrolysis and combustion. They developed a model for polycyclic aromatic hydrocarbons (PAH) and soot formation, in which the PAH molecular mass growth occurs by way of a two-step process involving hydrogen abstraction to activate the aromatic molecule followed by subsequent acetylene addition. Cyclization to the next highest order ring occurs when the sequence, H-abstraction followed by acetylene

addition ortho to ethynyl substituent is repeated (HACA mechanism). Then, the formation of primary soot particles occurs by coagulation of larger structures thus switching from the molecular scale of the order of a few angstroms, to the particle dimensions of the order of 10 nm. Surface growth by gas-to-particle addition at high temperature is considered to contribute a major part of the final soot concentration [5].

However, the transformation from low-molecular-weight organic gas phase species to particulate matter is not well understood because high-molecular-weight carbonaceous species formed during this process are difficult to analyze with certainty by conventional methods. Recent advances in experimental and modeling investigations in combustion have shown that a much larger amount of carbonaceous material, besides soot and GC-identifiable PAHs, is emitted in form of organic carbon (tar-like material) than were thought some years ago [6, 7]. A systematic characterization of the tar-like material, employing a large array of chemical and spectroscopic techniques [6–9], showed that tar is made up of high-molecular-weight com-

* Corresponding author. E-mail: violi@eng.utah.edu

¹ Also at the Department of Chemical Engineering, Università di Napoli "Federico II," Naples, 80125, Italy.

pounds in which aliphatic and aromatic character functionalities coexist. Tar is formed quite early in the soot pre-inception zone of flames and with a high formation rate. This organic material is initially transparent in the visible range, and shows ultraviolet spectroscopic properties [10, 11] compatible with two-, three-ring aromatics.

In order to explain these results one needs to invoke new reaction mechanisms for the formation of this material, not taken into account before. Considering the experimental evidences described above, D'Anna and Violi [12, 13] have proposed a new model for the formation of high-molecular-mass compounds and soot in slightly sooting flames [14]. Aromatics are rapidly formed in the main flame region through the combination of resonantly stabilized radicals; they grow up to 2-, 3-rings attaining a concentration level in flames comparable to the total concentration of soot, PAHs, and high-molecular-mass aromatics [14, 15]. As a consequence, the formation of high-molecular-mass aromatics and soot are considered just a rearrangement of PAHs. Soot inception then consists of the progressive aromatization of the initial structures through H-atom abstraction processes. The abstractions of H-atoms create additional double bonds and consequently fused aromatic rings in the cluster of tar-like material, with the increased extension of aromatic islands inside the structure [14]

This pathway for the formation of aromatic structures provides a parallel route to that of the classical HACA mechanism, and it may be favored during the early molecular growth process. In fact, recent experimental results obtained by D'Alessio et al., [16] assess the relevance of surface growth mechanism in the formation of soot and high-molecular-mass structures in premixed flames. The authors concluded that in slightly sooting flame conditions the processes of soot inception and mass growth do not involve surface growth by acetylene addition via the HACA mechanism. Instead, soot formation occurs through the rearrangement of a large amount of transparent (in the visible) particulate material that is formed by fast reactions among small PAH before soot inception. However, in richer flames, surface growth by means of gas-phase compounds such

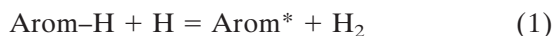
as acetylene becomes the dominant contributor to soot mass addition.

Therefore, it is important to identify key pathways for the molecular weight growth in conditions where the surface growth is not significant. These specific conditions are particularly relevant to practical systems. In fact, although the mass of visible transparent particles (tar) is lower than that of particles in the richer region, the number concentration is significant.

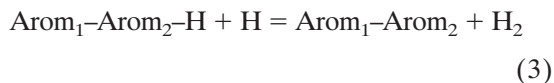
In this paper a molecular-level analysis for understanding the products of molecular weight growth is reported in order to determine the kinetic feasibility of the new proposed pathway, which provides a parallel route to that of the classical HACA mechanism.

MODEL FORMULATION

High-molecular-mass compounds can be formed in a sequence of chemical reactions that begins with the formation of radicals by H-abstraction from aromatic compounds:



The resulting radical furnishes higher aromatics through either a two-step reaction (radical-molecule reaction):



where $\text{Arom}_1\text{-Arom}_2\text{-H}$ represents an intermediate formed through an addition reaction, or a direct addition to another aromatic radical (radical-radical reaction):

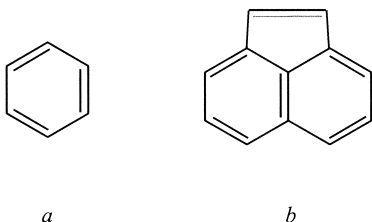


Iteration of this mechanism followed by rearrangement of the carbon framework ultimately leads to the formation of high-molecular-mass compounds.

The notion of the aromatic + aromatic pathway and their importance for PAH growth, is not new in the literature, i.e., Badger et al., [17], Graham et al., [18], Frenklach and co-workers [2, 3, 19, 20], Mauss et al., [21], and Bohm et al.,

[22], but the distinguishing features of the model here presented, lie in the chemical specificity of the routes proposed.

The reactions above described are analyzed in detail: two classes of compounds were considered: aromatics with 6 π -electron, i.e., benzene, naphthalene, and aromatics with conjugated double bonds, i.e., acenaphthylene, indene. The reactants chosen are: *a*) benzene (C_6H_6) belonging to the first class of aromatics (Arom₁-H); and *b*) acenaphthylene ($C_{12}H_8$) belonging to the second group (Arom₂-H).



The reasons for choosing these classes of compounds follow. Different studies have shown that polycyclic aromatic hydrocarbons with peripherally fused five-membered rings (CP-PAH), which include acenaphthylene, play key roles in the flame formation chemistry of soot [23, 24] and fullerenes [25]. The first proposal of the importance of acenaphthylene comes from a computational study by Frenklach et al. [1, 26] and theoretical analyses reported later [27, 28] extend further a possible role of peripherally fused five-membered rings.

Relative to other PAH, CP-PAHs demonstrate a greater facility in undergoing certain kinds of reactions, such as isomerization involving intramolecular rearrangement [29, 30], which is due to the fact that fusion of cyclopentane ring alters the electronic properties of PAH, as demonstrated by differences in resonance energy [31] and measured differences [32] in ultraviolet-visible absorption, fluorescence. CP-PAHs have been widely found in combustion systems, (e.g., ultraviolet, Lafleur et al., [33]). They have been observed as pyrolysis products of anthracene [34, 35], pyrene [36], and benzene [37], and as combustion products of benzene [38], ethylene [25], and ethylene-naphthalene [39] mixtures. Wornat et al. [40] pyrolyzed brown coal and through the analysis of the product tar, they identified different CP-PAH.

In a following work [41] the same group analyzed the condensed phase products from the fuel rich combustion of bituminous coal primary tar. Out of 10 and 8 CP-PAH, respectively, identified in the two works, acenaphthylene was found to be the most abundant under all the conditions investigated (26.5 mass percent of 1000°C tar sample). It has also been demonstrated that starting from acenaphthylene, the concentration of PAH decreases on the average by one order of magnitude with an increase in mass of 60 to 80 amu, rather independent of their absolute concentrations and of the combustion source [42].

This paper focuses on the application of quantum mechanical methods, particularly by using density functional theory calculations, to identify possible reaction pathways leading from benzene and acenaphthylene to higher aromatics.

CALCULATION PROCEDURE

The geometries of reactants as well as intermediates, transition states, and products have been optimized by using the hybrid density functional B3LYP method (i.e., Becke's three-parameter nonlocal exchange functional [43–45] with the nonlocal correlation function of Lee et al. [46]), with the 6–31G(d,p) basis set [47].

Vibrational frequencies of all species involved in the reaction were calculated using the optimized geometries at the B3LYP/6–31G(d,p) level and they have been used for characterization of the stationary points and calculation of zero-point energy (ZPE) corrections. All the energies cited below include ZPE corrections in units of Kcal/mol. The stationary points were identified by the number of imaginary frequencies (NIMF) with NIMF = 0 for a stable species and NIMF = 1 for a transition state.

All the calculations have been performed by using the Gaussain 98 program [48]. Reaction rate are calculated with TheRate code (THEoretical RATEs) [49] using the transition state theory. The thermal rate coefficient is expressed as:

$$k(T) = \kappa(T)\sigma \frac{k_B T}{h} \frac{Q^\ddagger(T)}{\Phi^R(T)} e^{\{-\Delta V^\ddagger/k_B T\}}$$

where κ is the transmission coefficient accounting for the quantum mechanical tunneling effects, σ is the reaction symmetry number, Q^\ddagger and Φ^R are the total partition functions (per unit volume) of the transition state and reactant, respectively, ΔV^\ddagger is the classical barrier height, T is the temperature, and k_B and h are the Boltzmann and Planck constants, respectively.

RESULTS AND DISCUSSION

The structures computed by the B3LYP/6 to 31G(d,p) method for the reactants, benzene and acenaphthylene, are shown in Fig. 1.

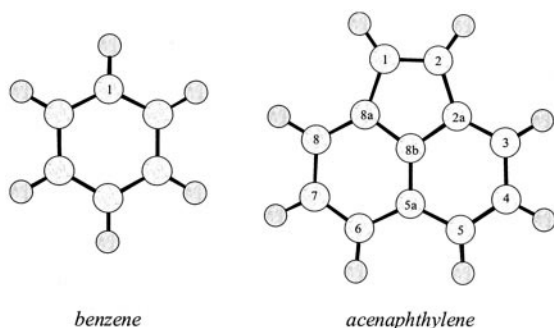


Fig. 1. Optimized structures for the reactants benzene and acenaphthylene.

Acenaphthylene belongs to the class of polycyclic hydrocarbons, which besides typical aromatic behavior can undergo reactions that are more typical of unsaturated rather than aromatic systems, i.e., 9,10-position in anthracene, 9,10-double bond in phenanthrene [50], 1,2-double bond in acenaphthylene. Specifically, these compounds are characterized by the pronounced reactivity and aliphatic character of this bond [51] and they react with electrophilic reagents by addition rather than by substitution [52]. This latter characteristic has been used in this analysis, as previously suggested [12–14].

The length of the double-bond C1–C2 in the five-membered ring for the optimized structure of acenaphthylene is 1.36 Å (Fig. 1) and it is larger than a typical carbon-to-carbon double

TABLE 1

The Calculated Energies of the Homolytic C–H Bond Cleavage (Reaction 1)^a

Parent arene	Site ^b	D_c^c	E_{ZPE}^d	D_o^e	
				this work	lit. [39]
Benzene	1	118.42	–8.24	110.18	110.7
Acenaphthylene	1	122.58	–5.64	116.93	
	3	118.18	–8.07	110.11	111.4
	4				110.1
	5				111.7

^a All energies in Kcal/mol.

^b The site of the hydrogen abstraction (carbon atoms numbered according to fig. 1).

^c D_c Dissociation energies.

^d E_{ZPE} Zero point vibrational energy.

^e D_o Ground-state dissociation energy.

bond (1.34 Å), but shorter than aromatic bonds (1.39 Å). This implies that the C1–C2 bond partially belongs to the aromatic sextets. Acenaphthylene is characterized by a high thermodynamic stability as stated by Stein and Fahr [53].

Table 1 reports the calculated energy of the homolytic C–H bond cleavage for the two reactants. The results obtained are in good agreement with the aryl–H bond dissociation energy obtained by Wang and Frenklach [54] using their own AM1-group correction method.

Results obtained for the phenyl radical serve as the gauge of accuracy of the present calculations. In agreement with the experimental evidence, using the electron-spin resonance spectrum [55], and the previous configuration interaction study [56] phenyl is found to be a σ -type radical with the 2A ground state. The computed $\langle \hat{S}^2 \rangle$ expectation value equals 0.757 (the exact value is 0.75) indicating only mild spin contamination. The calculated atomic charges and spin populations in the phenyl radical testify to the delocalization of unpaired electron in this species. For the phenyl radical the spin population of the H-abstracted C atom is 0.98, the two carbon atoms in the meta positions bearing most of the remaining spin. Charges on all atoms are close to zero and the most negative ones appearing at the carbons from which the hydrogen atoms have been removed.

Table 2 reports standard-state (298 K, $p = 1$

TABLE 2
Standard-State (298K, 1 atm) Thermodynamic Properties

Species	Formula	$C_p^o_{298}$ cal/mol/K		S^o_{298} cal/mol/K	
		this work	lit.	this work	lit.
Phenyl	C_6H_5	18.78	18.8 ^a 18.5 ^b	70212	69.0 ^a 68.6 ^b
Acenaphthylene	$C_{12}H_8$	35.28	36.9 ^d 36.4 ^b	86.095	87 ^c 86.4 ^b

^a Ref. [51].

^b Ref. [56].

^c Ref. [55].

^d Ref. [57].

atm) thermodynamic properties for the reactants in comparison with literature data. The calculated thermodynamic properties confirm the values obtained from more empirical approaches, e.g., the group contribution theory [51, 57], the semi-empirical quantum mechanical calculations by Wang and Frenklach [58], and the force-field approximation by Dorofeeva [59].

Reaction 1

Usually in the literature the 3-, or 5-acenaphthyl radicals have been considered in the kinetic models for aromatic growth. In particular in the HACA mechanism the acenaphthylene represents a key feature for PAH formation [1, 27], opening alternative channels for aromatic growth. For example, a direct formation of three-ring PAH, 4-phenanthryl initiated by the addition of 5-acenaphthyl radical to C_2H_2 (reaction pathways II in [27]).

As already mentioned, the site 1 in acenaphthylene structure (Fig. 1) has been chosen in this study because of its aliphatic character and because it reacts with electrophilic reagents (phenyl) giving addition reactions. To better emphasize this point, a deeper analysis of 3-, and 1-acenaphthyl radicals has been carried out. Figure 2 shows the relative energy ΔE (Kcal/mol) diagram for the H-abstraction to produce 1-acenaphthyl and H_2 , together with the optimized structures.

The breaking C–H bond length is 1.54 Å and the H–H length is 0.83 Å. The energetic barrier for the formation of the transition state is 13.25 kcal/mol. The computed energy barrier for 3-acenaphthyl formation starting from acenaph-

thylene and H is 10.4 kcal/mol, showing that at high temperature both radicals (3-, and 1-acenaphthyl) are widely produced, because the two energetic barriers can be easily overcome.

The reaction rate for the formation of 1-acenaphthyl + H_2 starting from acenaphthylene + H was calculated by using TheRate code (THEoretical RATEs) [47], with the transition state theory. The value obtained are reported in Fig. 3 in comparison with the reaction rate for the formation of 5-acenaphthyl used by Frenklach and coworkers [60].

Starting from 1200 K the reaction rate of 1-acenaphthyl reaches values comparable with those of the 5-acenaphthyl, indicating that the formation of 1-acenaphthyl may represent a significant pathway for molecular weight growth in combustion systems.

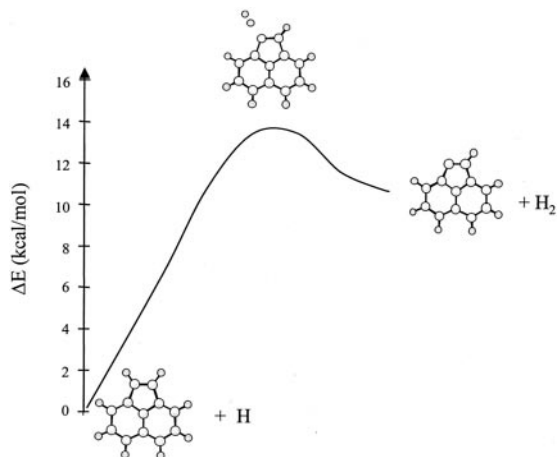


Fig. 2. Relative energy ΔE (kcal/mol) diagram for the reaction acenaphthylene + H = 1-acenaphthyl + H_2 , together with the optimized structures.

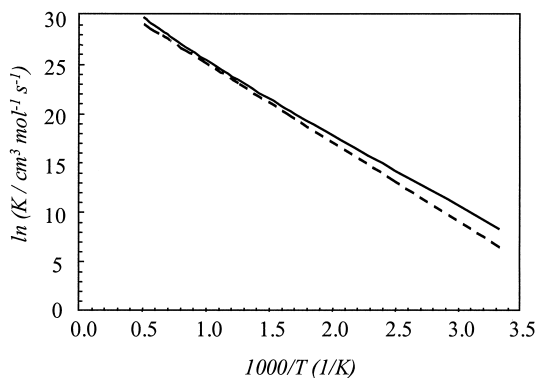


Fig. 3. Comparison between the predicted reaction rate for the reaction $C_{12}H_8 + H = 1-C_{12}H_7 + H_2$ (solid line) and $C_{12}H_8 + H = 5-C_{12}H_7 + H_2$ [60] (dashed line).

Reactions 2 and 3

For Reactions 2 and 3 we chose phenyl and acenaphthylene as $Arom_1^*$ and $Arom_2-H$, respectively, because of the importance of the attach of a radical to the double bond of five-membered-ring compounds.

The reaction of phenyl and acenaphthylene begins with the formation of the $C_6H_5C_{12}H_8$ ($Arom_1-Arom_2-H$ in Reaction 2) species, reported in Fig. 4 as structure 1. This intermediate is produced by the addition of phenyl to the double bond of acenaphthylene. A π bond is broken and a σ bond is formed with a length of 1.52 \AA ($C3-C3'$).

Steric hindrance brings about distortions from planarity in the geometry. An inspection of the optimized intermediate indicates that the two group planes are twisted to an angle of 118°

with respect to each other. This rotation effectively increases the distance between the H atoms situated in the bay region, minimizing the repulsion between them. At the same time, due also to the steric overcrowding, the H6 bonded to the sp^3 C of the five-member forms angles of 108° with the acenaphthylene plane (see Fig. 4). The new C-C bond is formed without encountering a barrier; the potential energy surface has an attractive character. The $C_6H_5C_{12}H_8$ has energy about 43 Kcal/mol lower than that of the reactants, at our B3LYP level. The unpaired electron is on the less substituted carbon, $C4'$, in the five-membered ring.

From this intermediate, it is possible to consider different pathways, i.e., unimolecular β -scission reactions either to release the 6 H-atom or to break the $2'-3'$ C-C bond, but in a rich combustion environment high concentrations of H-atom are available, so the intermediate can undergo an abstraction reaction. In particular H6 can be abstracted by the H atom. Structure 2 in Fig. 4 reports the product ($C_6H_5C_{12}H_7$) obtained after the H abstraction. The two electrons on the molecule ($C3'-C4'$) arrange themselves, giving back a double bond in the five-membered ring.

H-abstraction is exothermic because of the restoration of the resonance structures. The energy is 107 Kcal/mol lower than that of the reactants. The relief of steric overcrowding is accompanied by a flattening of molecular geometry and an increase of the stabilization through resonance. The calculated $C2-C3-C3'-C2'$ dihedral angle (Fig. 4, structure 2) is predicted to

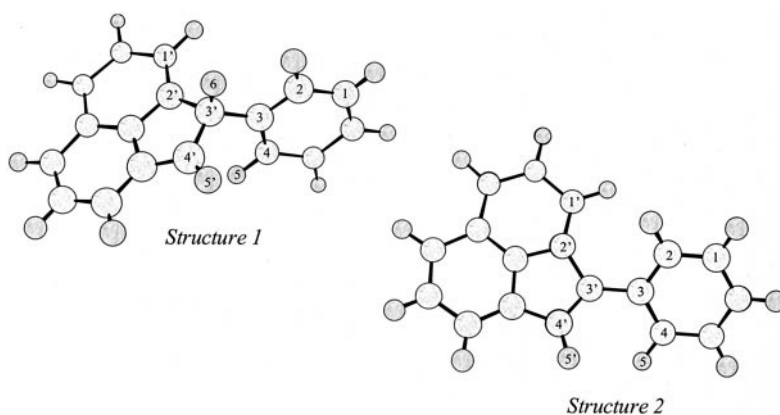


Fig. 4. Optimized structures for the intermediate $C_6H_5C_{12}H_8$ (structure 1) and the product $C_6H_5C_{12}H_7$ (structure 2).

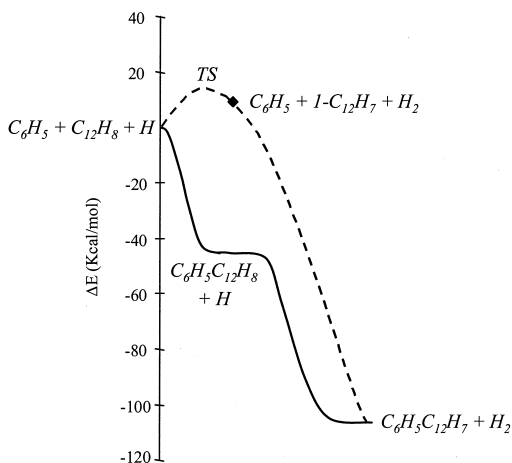


Fig. 5. Potential energy diagram at the B3LYP/6-31G(d,p) level for the Path 1 (solid line) and Path 2 (dashed line).

be 36° . The hydrogen abstraction is accompanied by a widening of the bond angle $C4'-C3'-C2'$ by $\sim 6.0^\circ$ and a concomitant shortening of the adjacent $C3'-C3$ bonds by $\sim 0.02 \text{ \AA}$, in good agreement with the observations reported by Cioslowsky et al., [61]. The relative energy ΔE (Kcal/mol) diagram for this route (Path 1) is reported in Fig. 5. The reference value considered for this graph is represented by the sum of the contribution of phenyl, acenaphthylene and H atom, the latter being involved in the second reaction step ($C_6H_5C_{12}H_8 + H = C_6H_5C_{12}H_7 + H_2$). The energies for all the species are summarized in Table 3.

For phenyl radical, the calculated parameters (vibrational frequencies and moments of inertia) were compared with available data obtained by Wang and Frenklach [58] using semiempiri-

TABLE 3

Relative Energies (Zero-Point-Energy-Corrected, in kcal/mol) for Species Involved in Reaction Path 1

Species	ZPE ^a	B3LYP/631G(d,p) ^b
C_6H_5	54.90	0.0
$C_{12}H_8$	100.18	0.0
H	0.0	0.0
$C_6H_5C_{12}H_8 + H$	156.92	-43.68
$C_6H_5C_{12}H_7 + H_2$	157.41	-107.71

^a ZPE calculated at B3LYP-6-31G(d,p) level.

^b The total energies (in Hartree) for phenyl, acenaphthylene, H-atom and H_2 are the following: -231.5692218, -462.1008247, -0.5002728, -1.1785393.

cal calculations and Madden et al., [62] employing the G2 M approach [63], showing a good agreement. At the B3LYP level no transition state has been identified for the Reaction 3 pathway to produce $C_6H_5C_{12}H_7 + H_2$ from $C_6H_5C_{12}H_8 + H$. This means that if the transition state exists, its energetic barrier is within the uncertainty of the level B3LYP (4-5 Kcal/mol). Because this value is very small, as the intermediate is formed, it rapidly forms the products ($C_6H_5C_{12}H_7 + H_2$), indicating that in the approximation of the steady state, the concentration of $C_6H_5C_{12}H_8$ is very low.

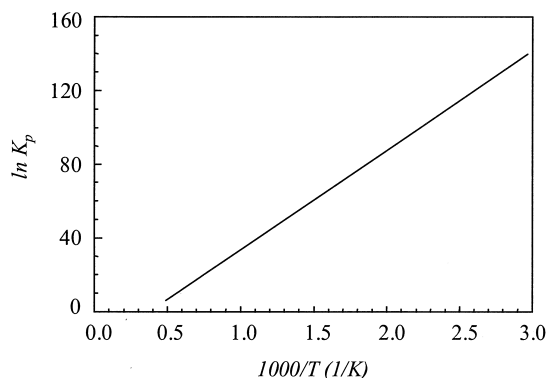


Fig. 6. Predicted equilibrium constant between reactants (C_6H_5 and $C_{12}H_8$) and products ($C_6H_5C_{12}H_7$ and H_2).

Equilibrium has been calculated between reactants (phenyl and acenaphthylene) and products ($C_6H_5C_{12}H_7 + H_2$). Figure 6 reports the equilibrium constant evaluated by using TheRate code.

In Reaction 2 (phenyl + acenaphthylene = $C_6H_5C_{12}H_8$) ΔS is negative: the system loses 6 degree of freedom (three translations and three rotations); in rx3 ($C_6H_5C_{12}H_8 + H = C_6H_5C_{12}H_7 + H_2$) the system gets two rotations for the formation of the linear molecule H_2 and ΔS is positive. The equilibrium constant approaches 1 ($\Delta G = 0$) for $T \sim 2000$ K. The reaction rate for the reaction between phenyl and acenaphthylene has been evaluated by using the collision theory and the result is reported in Fig. 7.

The calculated expression for the reaction rate is: $k(T) = 1.3E13 T^{0.5} \exp(6.95E-4/T)$. Further work will be conducted on this reaction to calculate the reaction rate by using varia-

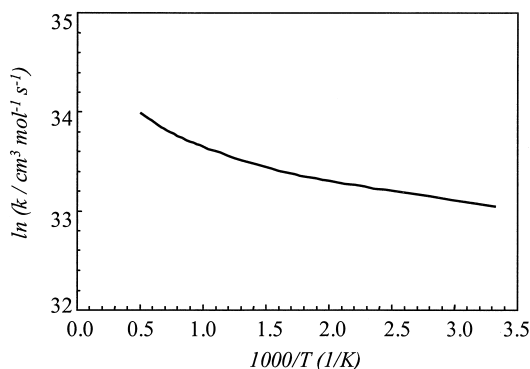


Fig. 7. Predicted reaction rate for the reaction between C_6H_5 and $C_{12}H_8$ evaluated using the collision theory.

tional transition state theory and to evaluate the rate coefficients at different pressure.

Reaction 4

Aside from Path 1, phenyl can react directly with 1-acenaphthyl radical. The product obtained from the addition reaction of these two radicals ($Arom_1^*$ and $Arom_2^*$) is the same as for the previous pathway and the structure is reported in Fig. 4 as structure 2. The electrons present on phenyl and 1-acenaphthyl radicals form a new C–C bond without encountering a barrier. The product has energy 117 kcal/mol lower than that of the two reactant radicals, as shown in Fig. 5. Table 4 reports the calculated energies for this second pathway.

The relative energy for this route (Path 2) is reported as dotted line in Fig. 5 together with the first analyzed pathway (solid line). The addition of $Arom_1^*$ and $Arom_2^*$ does not show

TABLE 4

Relative Energies (Zero-Point-Energy-Corrected, in Kcal/mol) for Species Involved in Reaction Path 2

Species	ZPE ^a	B3LYP/631G(d,p) ^b
C_6H_5	54.90	0
$C_{12}H_8$	100.18	0
H	0	0
TS + C_6H_5	154.26	13.25
$1-C_{12}H_7 + C_6H_5 + H_2$	155.83	11.63
$C_6H_5C_{12}H_7 + H_2$	157.41	-107.71

^a ZPE calculated at B3LYP-6-31G(d,p) level.

^b The total energies (in Hartree) for phenyl, acenaphthylene, H-atom and H_2 are the following: -231.5692218, -461.4052055, -0.5002728, -1.1785393.

any energetic barrier and the reaction rate for this pathway is expected to be similar to the one obtained in Path 1, with values close to the ones of the collision theory. The rate-limiting step for this pathway is represented by the H-abstraction from acenaphthylene, whose energetic barrier has been evaluated at ~ 14 Kcal/mol.

This result is not surprising: Wong and Radom [64] performed ab initio calculations at a variety of levels of theory for a number of prototypical radical addition reactions with a view to determining a level of theory suitable for predicting reliable barriers. By using the B3LYP method with 6-311G(d,p) basis set, they calculated the energetic barrier for the addition of CH_3^* to $CH_2 = CHX$ and their calculations show that when $X = CH_3$ the energetic barrier is 22.5 kJ/mol, but for $X = CHO$ the value drops down to 12.0 kJ/mol. This means that the transition state for the radical addition to the double bond can be stabilized by the π -bond network (resonance). The molecule produced with the reaction model proposed in this paper has much larger resonance effect and thus, the barrier is expected to be much lower.

The sequence of reactions (1–4) analyzed above can be considered as the first propagation step of a sequence that can be easily repeated, i.e., starting from the product reported in Fig. 4 as structure 2, through further H-atom abstractions, it is possible to get compounds with higher molecular mass. The energetic path will have the same trend as in the first sequence. The relative energetic barrier for the following steps will be smaller due to the greater stability of the higher molecular weight compounds. For example, the H abstraction from the product reported in Fig. 4 has been evaluated to have an energetic barrier of 10.7 Kcal/mol, which represents a lower value compared with that of H-abstraction from benzene or acenaphthylene (see Fig. 2).

A first validation for those new pathways comes from the results obtained by Mulholland et al., [65], who have studied polycyclic aromatic hydrocarbons growth from cyclopentadiene and indene. Addition of the cyclopentadienyl moiety to π bond produces a resonance-stabilized radical, which further reacts by one of two unimolecular channels. They concluded that pyrolytic growth of PAHs from indene and cyclopenta-

diene occurs predominantly by radical–molecule addition over a temperature range of 550 to 850°C, and they also proposed reaction pathways to account for the observed aromatic products found in their experiments, which resemble in the first part the mechanism here proposed.

CONCLUSIONS

In this paper computational support is provided for a reaction pathway of aromatic growth that parallels the HACA mechanism. Reaction routes are analyzed by using quantum mechanical density functional methods. High-molecular-mass compounds can be formed in a sequence of chemical reactions between aromatic compounds and compounds containing conjugated double bonds. The sequence begins with the H-abstraction from aromatic compounds to produce the corresponding radical, which then furnishes higher aromatics through either a two-step radical–molecule reaction or a direct radical–radical reaction addition. Iteration of this mechanism followed by rearrangement of the carbon framework ultimately leads to high-molecular-mass compounds. In this study these reactions have been analyzed in detail and possible reaction pathways are reported, using benzene and acenaphthylene as representative reactants.

The work presented in this paper adds new information to the general type of aryl–aryl and aryl–aromatic combination mechanism. The distinguishing features of the model presented lie in the chemical specificity of the routes proposed, where aromatic compounds attack the double bond of five-membered-ring PAH, forming resonantly stabilized radical intermediates, but more interesting is that the analysis reported shows the need of H abstraction from the Intermediate specie (structure 1 in Fig. 4) in order to get resonant stable compounds (structure 2 in Fig. 4). Without this added reaction the product would decompose to the reactants: the decrease in entropy in polymerization at high temperatures needs to be offset by the ΔH resulting from the hydrogen abstraction to provide a favorable ΔG for the forward reaction.

This research is funded by the University of Utah Center for the Simulation of Accidental Fires and Explosions (C-SAFE), funded by the Department of Energy, Lawrence Livermore National Laboratory, under subcontract B341493. Additional support was provided by the University of Naples "Federico II," Department of Chemical Engineering. A.V. thanks Hongzhi Zhang, Dr. Shaowen Zhang, and Anita Orendt for their technical assistance. The calculations presented in this paper were carried out at the Utah Center for High Performance Computing, University of Utah, which is acknowledged for computer time support.

REFERENCES

1. Frenklach, M., Clary, D. W., Gardiner, W. C., and Stein, S. E., *Proc. Combust. Inst.* 20:887 (1985).
2. Frenklach, M., Clary, D. W., Yuan, T., Gardiner, W. C., and Stein, S. E., *Combust. Sci. Tech.* 50:79 (1986).
3. Frenklach, M., Clary, D. W., Gardiner, W. C., and Stein, S. E., *Proc. Combust. Inst.* 21:1067 (1987).
4. Frenklach, M., and Warnatz, J., *Combust. Sci. Tech.* 51:265 (1987).
5. Frenklach, M., and Wang, H., in *Soot Formation in Combustion: Mechanisms and Models* (H. Bockhorn, Eds.), Springer-Verlag, Berlin, 1994, p. 265.
6. Ciajolo, A., D'Anna, A., Barbella, R., and Tregrossi, A., *Proc. Combust. Inst.* 25:679 (1994).
7. Lam, F. W., Longwell, J. P., and Howard, J. B., *Proc. Combust. Inst.* 23:1477 (1990).
8. Ciajolo, A., D'Anna, A., Barbella, R., Tregrossi, A., and Violi, A., *Proc. Combust. Inst.* 26:2327 (1996).
9. Bachmann, M., Wiese, W., and Homann, K.-H., *Proc. Combust. Inst.* 26:2259 (1996).
10. D'Alessio, A., D'Anna, A., D'Orsi, A., Minutolo, P., Barbella, R., and Ciajolo, A., *Proc. Combust. Inst.* 24:973 (1992).
11. Minutolo, P., Gambi, G., and D'Alessio, A., *Proc. Combust. Inst.* 27:1461 (1998).
12. Violi, A., and D'Anna, A., 21st Event of the Italian Section of the Combustion Institute, Italian Section of the Combustion Institute, Universita' Di Napoli "Federico II" Napoli, 26–29 May 1998, Ravello, Italy, p. 249.
13. D'Anna, A., and Violi, A., *Proc. Combust. Inst.* 27:425 (1998).
14. Violi, A., D'Anna, A., and D'Alessio, A., *Chemosphere* 42:27 (2000).
15. Violi, A., D'Anna, A., and D'Alessio, A., *Chem. Eng. Sci.* 54:3439 (1999).
16. D'Alessio, A., D'Anna, A., Minutolo, P., Sgro, L. A., and Violi, A., *Proc. Combust. Inst.* 28: 2547 (2000).
17. Badger, G. M., Jolad, S. D., and Spotswood, T. M., *Aust. J. Chem.* 20:1429 (1967).
18. Graham, S. C., Homer, J. B., and Rosenfeld, J. L. J., *Proc. R. Soc. London Ser. A* 344:259 (1975).

19. Appel, J., Bockhorn, H., and Frenklach, M., *Combust. Flame* 121:122 (2000).
20. Yoshihara, Y., Kazakov, A., Wang, H., and Frenklach, M., *Proc. Combust. Inst.* 25:941 (1994).
21. Mauss, F., Trilken, B., Breitbach, H., and Peters, N., in *Soot Formation in Combustion: Mechanisms and Models* (H. Bockhorn, Eds.), Springer-Verlag, Berlin, 1994, p. 325.
22. Böhm, H., Boenig, M., Feldermann, C., Jander, H., Rudolph, G., and Wagner, H. G., in *Soot Formation in Combustion: Mechanisms and Models* (H. Bockhorn, Eds.), Springer-Verlag, Berlin, 1994, p. 145.
23. Benish, T. G., Lafleur, A. L., Taghizadeh, K., and Howard, J. B., *Proc. Combust. Inst.* 26:2319 (1996).
24. McEnally, C. S., and Pfefferle, L. D., *Combust. Sci. Tech.* 131:323 (1998).
25. Lafleur, A. L., Howard, J. B., Taghizadeh, K., Plummer, E. F., Scott, L. T., Necula, A., and Swallow, K. C., *J. Phys. Chem.* 100:17421 (1996).
26. Frenklach, M., and Ebert, L. B., *J. Phys. Chem.* 92:561 (1988).
27. Frenklach, M., Moriarty, N. W., and Brown, N. J., *Proc. Combust. Inst.* 27:1655 (1998).
28. Frenklach, M., *Proc. Combust. Inst.* 26:2285 (1996).
29. Scott, L. T., and Roelofs, N. H., *J. Am. Chem. Soc.* 109:5461 (1987).
30. Howard, J. B., Longwell, J. P., Marr, J. A., Pope, C. J., Busby, W. F. Jr., Lafleur, A. L., and Taghizadeh, K., *Combust. Flame* 101:262 (1995).
31. DasGupta, A., and DasGupta, N. K., *Can. J. Chem.* 54:3227 (1976).
32. Jennessens, L. W., Sarobe, M., and Zwikker, J. W., *Pure Appl. Chem.* 68:219 (1996).
33. Lafleur, A. L., Howard, J. B., Plummer, E. F., Taghizadeh, K., Necula, A., Scott, L. T., and Swallow, K. C., *Poly. Arom. Comp.* 12:223 (1998).
34. Wornat, M. J., Sarofim, A. F., and Lafleur, A. L., *Proc. Combust. Inst.* 24:955 (1992).
35. Wornat, M. J., Vriesendorp, F. J. J., Lafleur, A. L., Plummer, E. F., Necula, A., and Scott, L. T., *Poly. Arom. Comp.* 13:221 (1999).
36. Mukherjee, J., Sarofim, A. F., and Longwell, J. P., *Combust. Flame* 96:191 (1994).
37. Marsh, N. D., Zhu, D., and Wornat, M. J., *Proc. Combust. Inst.* 27:1897 (1998).
38. Marsh, N. D., Wornat, M. J., Scott, L. T., Necula, A., Lafleur, A. L., and Plummer, E. F., *Poly. Arom. Comp.* 13:379 (2000).
39. Lafleur, A. L., Taghizadeh, K., Howard, J. B., Anacleto, J. F., and Quilliam, M. A., *J. Am. Soc. Mass Spectrom.* 7:276 (1996).
40. Wornat, M. J., Vernaglia, B. A., Lafleur, A. L., Plummer, E. F., Taghizadeh, K., Nelson, P. F., Li, C.-Z., Necula, A., and Scott, L. T., *Proc. Combust. Inst.* 27:1677 (1998).
41. Ledesma, E. B., Kalish, M. A., and Wornat, M. J., *Energy Fuels* 13:1167 (1999).
42. Homann, K. H., *Proc. Combust. Inst.* 20:857 (1984).
43. Becke, A. D. *J. Chem. Phys.* 96:2155 (1992).
44. Becke, A. D. *J. Chem. Phys.* 97:9173 (1992).
45. Becke, A. D. *J. Chem. Phys.* 98:5648 (1993).
46. Lee, C., Yang, W., and Parr, R. G., *Phys. Rev. B.* 37:785 (1988).
47. Hebre, W., Radom, L., Schleyer, P., R., and Pople, J. A., *Ab initio Molecular Orbital Theory*. Wiley, New York, 1986.
48. Frisch, M. J., Trucks, G. W., Schlegel, H. B., et al., *Gaussian 98, Revision A.7*. Gaussian, Inc., Pittsburgh, 1998.
49. Duncan, W. T., Bell, R. L., and Truong, T. N., *J. Computat. Chem.* 19:1039 (1998).
50. Garratt, P. J., *Aromaticity*. Wiley, New York, 1986.
51. Clar, E., *The Aromatic Sextet*. Wiley, London, 1972.
52. Badger, G. M., *Aromatic Character and Aromaticity*. Cambridge University Press, London, 1969.
53. Stein, S. E., and Fahr, A., *J. Phys. Chem.* 89:3714 (1985).
54. Wang, H., and Frenklach, M., *J. Phys. Chem.* 97:3867 (1993).
55. Kasai, P. H., Clark, P. A., and Whipple, E. B., *J. Am. Chem. Soc.* 92:2640 (1970).
56. Berkowitz, J., Ellison, G. B., and Gutman, D. J., *J. Phys. Chem.* 98:2744 (1994).
57. Stein, S. E., and Barton, B. D., *Thermochim. Acta* 44:265 (1981).
58. Wang, H., and Frenklach, M., *J. Phys. Chem.* 98:11465 (1994).
59. Dorofeeva, O. V., *Thermochim. Acta* 102:59 (1986).
60. Appel, J., Bockhorn, H., and Frenklach, M., *Combust. Flame* 121:122 (2000).
61. Cioslowski, J., Liu, G., Martinov, M., Piskorz, P., and Moncrieff, D., *J. Am. Chem. Soc.* 118:5261 (1996).
62. Madden, L. K., Moskaleva, L. V., Kristyan, S., and Lin, M. C., *J. Phys. Chem. A* 101:6790 (1997).
63. Mebel, A. M., Morokuma, K., and Lin, M. C., *J. Chem. Phys.* 103:7414 (1995).
64. Wong, M. W., and Radom, L., *J. Phys. Chem. A* 102:2237 (1998).
65. Mulholland, J. A., Lu, M., and Kim, D.-H., *Proc. Combust. Inst.* 28:2593 (2000).

Received 1 November 2000; revised 26 April 2001; accepted 6 May 2001